Geofísica Internacional (1998), Vol. 37, Num. 2, pp. 55-70

Feedback effects of atmospheric CO_2-induced warming

Julián Adem[1,2] and René Garduño[2]
[1] Member of El Colegio Nacional, México.
[2] Centro de Ciencias de la Atmósfera, UNAM, México, DF, México.

Received: November 15, 1997; accepted: February 11, 1998.

RESUMEN

Utilizando un modelo termodinámico del clima, se lleva a cabo un estudio sobre los cambios en la temperatura y precipitación debidos a una duplicación del contenido atmosférico de CO_2 y sobre la importancia relativa, en la temperatura, de los mecanismos de retroalimentación asociados con los aumentos de vapor de agua, nieve-hielo y nubosidad. Los factores de retroalimentación del modelo termodinámico son similares a los de los modelos de Hansen *et al*. (1984) y Schlesinger (1986). El factor de retroalimentación de los tres mecanismos combinados es 4.0. Los resultados dependen en forma importante del contenido de vapor de agua en la banda del CO_2 (12-19μ). El aumento de temperatura debido a la duplicación de CO_2 es igual a 1.2° C cuando existe vapor de agua en dicha banda y es igual a 3.5° C cuando no hay vapor de agua. Los resultados muestran que una posible causa de las grandes diferencias en las soluciones obtenidas con diferentes modelos podrían ser las discrepancias en la cantidad y distribución del vapor de agua en la atmósfera, y en el tratamiento de su efecto en la banda del CO_2.

PALABRAS CLAVE: CO_2 atmosférico, calentamiento, retroalimentadores.

ABSTRACT

Using a thermodynamic climate model, temperature and precipitation changes due to a doubling of atmospheric CO_2 content, including the corresponding feedback temperature increases of water vapor, snow-ice, and cloudiness, are evaluated. The feedback factors of the thermodynamic model are similar to those of Hansen *et al.* (1984) and Schlesinger (1986). The feedback factor of all three mechanisms combined is 4.0. The results depend mainly on the content of water vapor in the CO_2 band (12-19μ). The temperature increase due to a doubling of CO_2 is 1.2° C when there is water vapor in the band, and 3.5° C when there is no water vapor. Therefore, a possible cause of the strong differences in the solutions obtained by different models is the discrepancy in the amount and distribution of water vapor in the atmosphere, and in the treatment of its effect in the CO_2 band.

KEY WORDS: Atmospheric CO_2, warming, feedbacks.

1. INTRODUCTION

The effect on the surface temperature of an increase in atmospheric CO_2 has been discussed by many authors, using a variety of models. Tricot and Berger (1987), extended Schlesinger's (1984) summary. Figure 1, reproduced from their paper, includes our earlier results (Adem and Garduño, 1984). The figure shows the change of surface air temperature for a doubling of CO_2 concentration in the atmosphere, according to different authors, using energy balance models (EBMs), radiative-convective models (RCMs) and general circulation models (GCMs). The values vary from 0.5° to 5.5° C. It is essential to carry out numerical experiments to determine the possible causes of such a wide range of values.

Using the Adem Thermodynamic Climate Model (ATM), we carry out numerical experiments to evaluate the feedback effects for increases of the atmospheric water vapor, snow-ice on oceans and continents, and cloud cover, due to a doubling of the CO_2. We use a version of ATM with an annual cycle of snow-ice (Adem, 1982), which has been modified to conserve the water in the system (Adem and Garduño, 1984).

In the earlier experiments (Adem and Garduño, 1982, 1984) we had used different estimates (Yamamoto and Sasamori, 1958, 1961) for the emission spectrum of CO_2, and the H_2O feedback was not included. In the present work we use new spectra (Smith, 1969; Garduño and Adem, 1988) of CO_2 and H_2O for wavelengths longer than 12μ, and a Ramanathan (1976) type spectrum for wavelengths shorter than 12μ for H_2O. As for the cloud-temperature feedback, instead of the former treatment (Adem, 1982), we now use a parameterization of relative humidity as a function of the horizontal extent of cloudiness (Adem, 1967), plus the assumption that the relative humidity remains fixed (Garduño and Adem, 1993). Finally, the snow-ice-temperature feedback is performed by coupling the 0° C computed surface (ocean or continental ground) isotherm to the boundary of the horizontal extent of snow-ice (Adem, 1982).

The model generates tropospheric, surface ocean, and continental ground temperatures, as well as the precipitation.

The region of integration of ATM includes nearly all Northern Hemisphere (NH). The variables are computed monthly.

2. DESCRIPTION OF THE MODEL

The model consists of an atmospheric layer of about 9

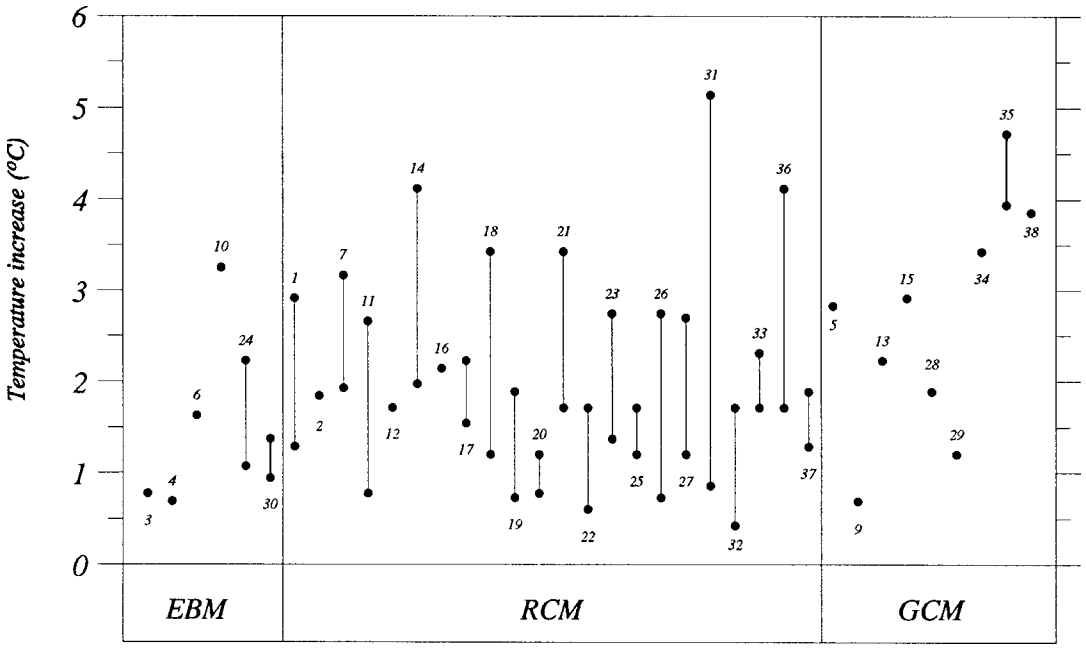

Fig. 1. The change of surface air temperature (in ° C) for doubling the CO_2 concentration as simulated by energy balance models (EBMs), radiative-convective models (RCMs) and general circulation models (GCMs). This figure was adapted and modified by Tricot and Berger (1987) from a previous one by Schlesinger (1984). The results are numbered in chronological order: 1 Manabe and Wetherald (1967), 2 Manabe (1971), 3 Rasool and Schneider (1971), 4 Weare and Snell (1974), 5 Manabe and Wetherald (1975), 6 Temkin and Snell (1976), 7 Augustsson and Ramanathan (1977), 8 Rowntree and Walker (1978), 9 Ohring and Adler (1978), 10 Ramanathan *et al*. (1979), 11 Hunt and Wells (1979), 12 Ackerman (1979), 13 Potter (1980), 14 Wang and Stone (1980), 15 Manabe and Wetherald (1980), 16 Ramanathan (1981), 17 Charlock (1981), 18 Hansen *et al*. (1981), 19 Hummel and Kuhn (1981a), 20 Hummel and Kuhn (1981b), 21 Hummel and Reck (1981), 22 Hunt (1981), 23 Wang *et al*. (1981), 24 Chou *et al*. (1982), 25 Hummel (1982a), 26 Hummel (1982b), 27 Lindzen *et al*.(1982), 28 Schlesinger (1983), 29 Washington and Meehl (1983), 30 Adem and Garduño (1984), 31 Wang *et al*. (1984), 32 Somerville and Remer (1984), 33 Lal and Ramanathan (1984), 34 Washington and Meehl (1984), 35 Hansen *et al*. (1984), 36 Ou and Liou (1985), 37 Gutowski *et al*. (1985), and 38 Wetherald and Manabe (1986).

km high which includes a cloud layer, an oceanic layer of 50 to 100m in depth and a continental layer of negligible depth. The basic prognostic equations are those of conservation of thermal energy as applied to this atmosphere—ocean—continent system.

The vertically integrated equation of thermal energy for the atmospheric layer is (Adem, 1965a):

$$c_v a_o \frac{\partial T_m'}{\partial t} + A_D + W_T = E_T + G_5 + G_2 \qquad (1)$$

where t is the time, T_m' is the deviation of the mean atmospheric absolute temperature from a constant value T_{mo}, $T_{mo} >> T_m'$; c_υ is the specific heat of air at constant volume. And

$$a_o = \int_o^H \rho_o^* dz, \quad A_D = c_\upsilon M_a \cdot \nabla T_m' \text{ and } M_a = \int_o^H \rho_o^* \mathbf{v}_H^* dz,$$

where H is the constant height of the model atmosphere (i.e. the top of the troposphere), ∇ is the two-dimensional horizontal gradient operator, z is the vertical coordinate and ρ^* is the density given by

$$\rho^* = \rho\,(1+\beta\,(H-z)\,/\,(T_m - \beta H/2))^{\gamma-1}$$

where

$$\gamma = \frac{g}{R\beta} \quad .$$

$T_m = T_{mo} + T_m'$, ρ is a fixed constant density at $z = H$, β is the lapse rate used in the atmospheric layer, g is the acceleration of gravity, R is the gas constant, $\mathbf{v}_H^*$ is the horizontal component of the wind, and ρ_o^* is the value of ρ^* obtained by replacing T_m by T_{mo}.

In (1) E_T is the rate at which energy is added by radiation, G_2 is the rate at which heat is added by vertical turbulent transport from the surface, and G_5 is the rate at which heat is added by condensation of water vapor in the clouds. The local rate of change of thermal energy is $c_v a_o \partial T_m'/\partial t$, the advection of thermal energy by the mean wind is A_D and the horizontal transport of heat by transient eddies is W_T.

The equation used for the ocean layer (Adem, 1970a) is

$$h\rho_s c_s \frac{\partial T_s'}{\partial t} = E_s - G_2 - G_3 \qquad (2)$$

where $T_s' = T_s - T_{so}$ is the departure of the surface ocean absolute temperature T_s from a constant value T_{so}, where T_{so} >>

T_s', ρ_s is a constant density and c_s is the specific heat, h is the depth of the layer, E_s is the rate at which energy is added by radiation, G_2 is the rate at which sensible heat is lost to the atmosphere by vertical turbulent transport, and G_3 is the rate at which heat is lost by evaporation.

Over continents, (2) reduces to

$$O = E_s - G_2 - G_3 \ .$$

If we use parameterizations for E_T, E_s, G_2, G_5, G_3, A_D and W_T, then the different components that appear in (1) and (2) are expressed as linear functions of T_s' and T_m' or of their first and second derivatives with respect to the map coordinates x and y.

The parameterizations of the heating and transport components require the use of physical laws and conservation principles supplemented by observed data, so that the formulas used are semi–empirical.

3. PARAMETERIZATION OF ATMOSPHERIC RADIATION

Using a method similar to the one developed by Adem (1962) and Adem and Garduño (1982, 1984) we obtain:

$$\begin{aligned} E(T) = \sigma T^4 &- (1-a_1)F(T, 2\mu, 8.3\mu) \\ &- (1-a_2)F(T, 8.3\mu, 12\mu) \\ &- \sum_{n=12}^{18}(1-a_n)F(T, n\mu, (n+1)\mu) \end{aligned} \qquad (3)$$

where $E(T)$ is the atmospheric emission at temperature T for clear sky. The function $F(T, \lambda_1, \lambda_2)$ is given by

$$\begin{aligned} F(T,\lambda_1,\lambda_2) &= \int_{\lambda_1}^{\lambda_2} c_1\lambda^{-5}e^{-c_2/\lambda T}d\lambda \qquad (4) \\ &= \left[c_1 e^{-c_2/\lambda T}\left(\frac{T}{c_2\lambda^3} + \frac{3T^2}{c_2^2\lambda^2} + \frac{6T^3}{c_2^3\lambda} + \frac{6T^4}{c_2^4}\right)\right]_{\lambda_1}^{\lambda_2} \end{aligned}$$

where λ is the wavelenght, σ = 8.215 x 10^{-10} cal cm^{-2} (° K)$^{-4}$ min^{-1}, c_1 = 5.538 x 10^5 cal $\mu^4 cm^{-2}$ min^{-1} and c_2 = 14350μ °K.

In formula (3), the coefficients a_1 and a_2 are the absorptivity values due to H_2O, computed as in Ramanathan (1976), for the intervals (2μ, 8.3μ) and (8.3μ, 12μ), respectively; and a_{12}, a_{13}, a_{14}, a_{15}, a_{16}, a_{17} and a_{18} are the absorptivities due to CO_2 and H_2O, which are computed using Smith (1969) and Adem (1967) in the way described by Garduño and Adem (1988).

The integral in Eq. (4) is evaluated by Boltzmann's formula which is an approximation for small values of λ in the exact formula due to Planck. The error increases as λ increases, so that it is less than 0.1%, 0.9%, 2.9% and 5.0% for λ smaller than 8μ, 12, 16, and 19μ, respectively.

If $T = T_o + T'$, where $T_o >> T'$, Eq. (3) becomes (Adem, 1962)

$$E(T) = E(T_o) + \left(\frac{\partial E}{\partial T}\right)_{T=T_o} T' \ . \qquad (5)$$

Since T is in degrees Kelvin, T' is for atmospheric temperatures usually much smaller than T_o. Therefore the linear formula (5) is a good approximation to (3) and is used in the model.

We assume that there is a cloud layer, of variable horizontal extent $\in$, that radiates as a black body with a temperature of 261° K. Furthermore we assume that the surface of the Earth radiates as a black body and that it absorbs short wave radiation from the sun and sky according to the Savino—Ångström formula. Making a balance of radiation as in Adem (1962), we obtain

$$E_T = A_2''T_m' + (A_3 + \in D_3)T_s' + A_6 + \in D_6' + (a_2' + \in b_3)I \qquad (6)$$

and

$$E_s = B_2''T_m' + B_3T_s' + B_6 + \in B_7 + (Q+q)_o[1-(1-k)\in](1-\alpha) \qquad (7)$$

where A''_2, A_3, A_6, D_3, D_6', B_2'', B_3, B_6, B_7 are constants; a_2' and b_3 are functions of latitude and season; $(Q+q)_o$ is the total radiation received by the surface with clear sky, k is a function of latitude, I is the insolation, and α is the surface albedo (Adem, 1962, 1964a, 1964b).

4. ABSORPTIVITY FOR WAVELENGTHS LESS THAN 12μ

On computing a_1 and a_2 in Section 3, and according to Kirchhoff's law, we use Ramanathan's (1976) emissivity formulas:

$$a_1 = 0.59\left(\frac{T_1}{T}\right)^{1/4}\left(1 - \frac{0.5}{1+b_1\sqrt{U_1}} - \frac{0.5}{1+b_2\sqrt{U_1}}\right) \qquad (8)$$

and

$$a_2 = [0.272 + d_2(T - T_2)][1 - \exp(d_1U_2)], \qquad (9)$$

where

$$U_1 = \int \frac{P}{P_o}\sqrt{\frac{T_1}{T}}\,dU_A \qquad (10)$$

and

$$U_2 = \frac{1}{e_o}\int (e + cP)dU_A \ . \qquad (11)$$

The integrals in (10) and (11) are taken vertically across the atmosphere, although their integrand is significant only in the lowest few kilometers. U_A is the water vapor amount in cm if it was a liquid at STP conditions (some authors call this unit cm-atm; both are numerically the same as g cm^{-2}). U_A is also called precipitable water; T and P are the atmospheric temperature and pressure, respectively; e is the par-

tial pressure of water vapor, P_o is the STP pressure (1.013 x 10^6g cm^{-1} s^{-2}); and T_1, T_2, b_1, b_2, c, d_1, d_2 and e_o are constants.

In order to evaluate (10) and (11), we express all variables in terms of T; for this purpose we use the following formulas from ATM (Adem, 1967; Garduño and Adem, 1988):

$$dU_A = R_1 F(T)\, dT \tag{12}$$

and

$$P = P_a\left(\frac{T}{T_a}\right)^{\gamma} \quad , \tag{13}$$

where

$$F(T) = \left(0.5 \in + \sum_{i=0}^{2} f_i T^i\right) \sum_{i=-1}^{3} n_i T^i \quad .$$

T_a and P_a are the temperature and pressure at the bottom of the atmosphere.

$$R_1 = \frac{0.622}{\rho_a R \beta}$$

$$f_o = \sum_{i=0}^{2} A_i \left(\frac{T_a}{\beta}\right)^i$$

$$f_1 = -\frac{1}{\beta}\left(A_1 + 2A_2\frac{T_a}{\beta}\right)$$

$$f_2 = \frac{A_2}{\beta^2}$$

$\rho_a, A_o, A_1, A_2, n_{-1}, n_o, n_1, n_2$ and n_3 are constants.

Furthermore,

$$e(T) = F(T)\, T. \tag{14}$$

Now, we substitute (12) and (13) in (10), obtaining

$$U_1 = k_1 \int_{T_H}^{T_a} T^{\eta} F(T) dT \tag{15}$$

where

$$k_1 = R_1\sqrt{T_1 T_a^{\gamma}}$$
$$T_H = T_a - \beta H$$
$$\eta = \gamma - 0.5 \quad .$$

Substituting (12), (13) and (14) in (11), we get

$$U_2 = \frac{R_1}{e_o}\int_{T_H}^{T_a}\left[cP_a\left(\frac{T}{T_a}\right)^{\gamma} + F(T)T\right]F(T)dT \ , \tag{16}$$

where U_1 and U_2 from (15) and (16) are in cm.

The climatic parameters are taken as annual and global averages; these (normal) values are:

T_a = 288°K

$P_a = P_o$

β = 6.5 x 10^{-5}°K cm^{-1}

$\in$ = 0.5

H = 9 x 10^5 cm

For T, in (8) and (9), we take the value of the "equivalent" temperature for H_2O, computed by Garduño and Adem (1988), which is 275.6° K.

The values of U_1 and U_2 from (15) and (16) are substituted in (8) and (9) to get the absorptivity from 2 to 12μ. These values of a_1 and a_2 yield the basic (normal) atmospheric spectrum (in that interval), which is representative of the whole Earth and full year, corresponding to the present global and annual averages of the climatic parameters. This spectrum interacts with the climate through these five parameters. When the climate changes (for example, as a consequence of an increment in the atmospheric CO_2 content, externally imposed, as in the experiments presented in this paper), T_a, β and $\in$ are allowed to increase. To compute the increments (anomalies) T_aDN, βDN and $\in DN$ we assume P_a and H fixed; nevertheless P is allowed to increase by means of T_a in (13). Using the increased (abnormal) values of T_a, β and $\in$, the corresponding increased (abnormal) values of the absorptivities a_1 and a_2 are computed.

The atmospheric spectra, computed as explained in sections 3 and 4, are shown in Figure 2, for present and doubled CO_2 amounts. Part A is the spectrum for CO_2 alone, B is for H_2O and part C for both gases combined.

5. OTHER PARAMETERIZATIONS

As in previous papers (Adem, 1982; Adem and Garduño, 1984), we use for G_2, G_3 and G_5 the formulas

$$G_1 = G_{2N} + G_2DN \tag{17}$$

$$G_3 = G_{3N} + G_3DN \tag{18}$$

$$G_5 = G_{5N} + G_5DN \tag{19}$$

where G_{2N}, G_{3N} and G_{5N} are prescribed seasonal climatological normal values, and G_2DN, G_3DN and $G_{5N}DN$ are the corresponding anomalies which are computed internally in the model.

The conservation of water vapor in an atmospheric column of unit area requires that

$$G_3 - G_5 = LE' \tag{20}$$

where L is the heat of vaporization and E' includes the horizontal transport and the storage of water vapor terms (Adem, 1968).

Substituting (18) and (19) in (20) we find

$$(G_{3N} - G_{5N}) + (G_3DN - G_5DN) = L(E_N' + E'DN) \tag{21}$$

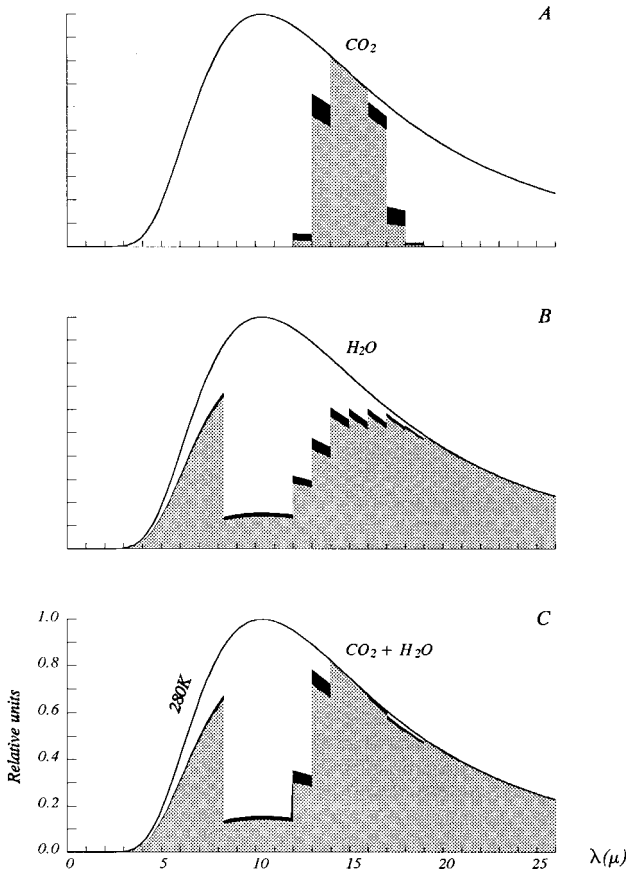

Fig. 2. Atmospheric emission spectra used in our models: normalized energy emitted as a function of wave length (λ). The shaded area is the energy emitted by the atmosphere for present CO_2 content, and the black area is the increase due to doubling the CO_2. Parts A and B are the spectra for CO_2 alone and for water vapor alone, respectively, and part C is the spectrum for both gases combined. The spectra are illustrated with the Planck's curve for 280° K, but this temperature is a variable in the models.

where E' is written as the sum of a normal value E_N' and an anomaly $E'DN$.

Equation (20) is assumed to be valid for normal values, therefore

$$G_{3N} - G_{5N} = LE_N' \quad . \tag{22}$$

Substracting (22) from (21),

$$G_3DN - G_5DN = LE'DN \quad .$$

We assume that

$$G_3DN = G_5DN \quad . \tag{23}$$

This assumption implies that the anomaly of transport and storage of water vapor is taken as zero. However, since G_{3N} and G_{5N} are prescribed so that (22) is satisfied, the normal value of the transport and storage (E_N') is retained. Therefore the equation of conservation of water vapor is satisfied under the assumption that $E'_N >> E'DN$.

For G_2DN we use the formula

$$G_2DN = K_3|V_{a_N}|[(T_s' - T_{s_N}') - (T_m' - T_{m^N}')] \ , \tag{24}$$

where T_{sN}' and T_{m_N}' are the computed normal values of T_s' and T_m', respectively; K_3 is a constant and $|V_{a_N}|$ is the prescribed normal surface wind speed. This linearized formula was derived by Clapp *et al*. (1965) and has been used in previous experiments (Adem, 1965a, 1982).

In these experiments we had used the formula

$$G_3DN = 2G_2DN \tag{25}$$

which implied a Bowen ratio of 2 for the anomalies.

For the horizontal wind the following formula is used (Adem, 1982):

$$\boldsymbol{v}_H^* = \boldsymbol{v}^*_{N_{ob}} + (\boldsymbol{v}^* - \boldsymbol{v}_N^*) \tag{26}$$

where $\boldsymbol{v}^*_{Nob}$ is the observed geostrophic wind and $\boldsymbol{v}^* - \boldsymbol{v}_N^*$ is the computed anomaly of the wind, in which the two components of $\boldsymbol{v}^*$ are computed from the formulas

$$u^* = -\frac{R}{fT}\left(T_o + (H-z)\left(\beta - \frac{g}{R}\right)\right)\frac{\partial T_m'}{\partial y_1} \tag{27}$$

$$v^* = \frac{R}{fT}\left(T_o + (H-z)\left(\beta - \frac{g}{R}\right)\right)\frac{\partial T_m'}{\partial x_1} \tag{28}$$

where u^* and v^* are the components along the x_1 and y_1 axes (x_1 to east, and y_1 to north), and f is the Coriolis parameter; also $T_o = T_{mo} - \beta H/2$.

To compute the components of the normal horizontal wind $\boldsymbol{v}^*_N$, Eqs. (27) and (28) are used with the normal value T_{mN} instead of T_m'.

The advection by mean wind (A_D) is given by Adem (1970b):

$$A_D = (F_8)_o J\left(T_m', p_{N_{ob}}\right) + \left(F_8''\right)_o J\left(T_m', T_{N_{ob}}\right) - \left(F_8'\right)_o J\left(T_m', T_{m_N}'\right) \tag{29}$$

where $(F_8)_o$, $(F_8')_o$ and $(F_8'')_o$ are constants and

$$T_{N_{ob}} = -\beta\left(H - H_{7N_{ob}}\right) + T_{7N_{ob}}$$

$$p_{N_{ob}} = p_{7N_{ob}}\left(T_{N_{ob}} / T_{7N_{ob}}\right)^{\gamma} \ ,$$

where $H_{7N_{ob}}$ is the normal observed 700mb height, $T_{7N_{ob}}$ is the normal observed 700mb temperature and $p_{7N_{ob}}$ = 700mb.

The horizontal turbulent transport is

$$W_T = -c_v a_o K \nabla^2 T_m' \tag{30}$$

where ∇^2 is the two-dimensional horizontal Laplacian operator and K is the "Austausch" coefficient, which is taken as a constant equal to 3 x $10^6 m^2 s^{-1}$. This value of K is of the same order of magnitude as for the migratory cyclones and anticyclones of the middle latitudes, which are considered as turbulent eddies (Defant, 1921; Clapp, 1970).

The precipitation anomalies are computed externally from the empirical formula (Clapp *et al*., 1965)

$$S = S_N + L\left[b(T_m' - T_{mN}') + d''\left(\frac{\partial T_m'}{\partial x} - \frac{\partial T_{mN}'}{\partial x} \right) + c''\left(\frac{\partial T_m'}{\partial y} - \frac{\partial T_{mN}'}{\partial y} \right) \right] \tag{31}$$

where S_N is the normal seasonal value, and b, d" and c" are functions of x, y and season.

A brief description of this formula is given by Adem (1996).

6. WATER VAPOR AND CLOUDINESS FEEDBACKS

In these experiments, the computation of the coefficients a_i(i = 1, 2, 12, 13, 14, 15, 16, 17, 18), in Eq. (3), which includes the water vapor feedback, is carried out as an average over the integration region and in the year instead of at each of the grid points and for each month, as follows:

First we obtain the coefficients a_i for the computation of the normal case, using the Smith (1969) formula for i = 12, 13, 14, 15, 16, 17, 18 as described by Garduño and Adem (1988).

The values used to compute a_i are

U_{BN} = 260 cm

U_{AN} = 2.4 cm

T_{sN} = 288°K

$P_{sN} = P_o$

β_N = 6.5°K km^{-1}

H = 9km

ϵ_N = 0.5

where U_{BN} is the normal (present) CO_2 content, U_{AN} is the normal atmospheric H_2O content, T_{sN} is the normal surface air temperature; P_{aN} is the normal surface air pressure, β_N is the normal lapse rate, and ϵ_N is the normal fractional cloudiness. The coefficients a_1 and a_1 are computed using the Ramanathan (1976) approach (Section 4).

For the abnormal case, we compute a_i for i from 12 to 18, in Eq. (3), using Smith's (1968) formula with the values

$U_B = 2U_{BN}$

$U_A = U_{AN} + U_A DN$

$T_s = T_{sN} + T_s DN$

$P_s = P_{sN} + P_s DN$

$\beta = \beta_N + \beta DN$

$\epsilon = \epsilon_N + \epsilon DN$

where U_B is twice the present atmospheric CO_2 content, and $U_A DN$, $T_s DN$, $P_s DN$, βDN and ϵDN are the increases, due to the doubling of the CO_2, of the atmospheric H_2O, the surface temperature, the surface pressure, the lapse rate and the horizontal extent of cloudiness, respectively.

The cloud cover ϵ is included as

$$\epsilon = \epsilon_N + \epsilon DN \tag{32}$$

where ϵ_N is the observed normal seasonal cloudiness and ϵDN is the internally computed anomaly which is given by

$$\epsilon DN = -\ 1.26 T_m DN \tag{33}$$

where ϵDN is in percent and $T_m DN$ in Kelvin degrees.

Eq. (33) is semi-empirical and is based on the assumption that the relative humidity remains fixed. The detailed derivation is given by Garduño and Adem (1993). This provides the cloud feedback, which is also evaluated as an average over the integration region and the year.

The surface albedo α is generated internally in the model by coupling the computed 0° C surface (continental ground or ocean) isotherm with the boundary of the snow—ice cover, as described by Adem (1981, 1982). This coupling yields the snow—ice—temperature feedback used in the present experiments.

7. METHOD OF SOLUTION

In (1), $\partial T_m'/\partial t$ is replaced by $(T_m' - T_{mp}')/\Delta t$, where T_{mp}' is the value of T_m' in the previous month and Δt is the time interval, taken as a month. Similarly, $\partial T_s'/\partial t$ in (2) is replaced by $(T_s' - T_{sp}')/\Delta t$, where T_{sp}' is the value of T_s' in the previous month.

Using these backward finite differences and substituting the parameterizations of the heating and transport terms (6), (7), (17), (18), (23), (24), (25), (29) and (30) in (1) and (2), the problem is reduced to solving two equations with two unknowns T'_m and T'_s. Eq. (2) can be combined with (1) to yield a single second-order elliptic differential equation in T_m':

$$K\nabla^2 T_m' + F_1 \frac{\partial T_m'}{\partial x} + F_2 \frac{\partial T_m'}{\partial y} + F_3 T_m' = F_4 \qquad (34)$$

where F_1, F_2, F_3 and F_4 are functions of the map coordinates and α; and F_4 is also a function of T_{mp}' and T_{sp}'.

We first compute the normal case, using normal initial and boundary conditions; then the abnormal case, using the abnormal initial and boundary conditions, and the computed normal fields on which, according to eqs. (24) and (29), the abnormal variables depend, namely on T_{s_N}', T_{m_N}', $\partial T_{m_N}'/\partial x$ and $\partial T_{m_N}'/\partial y$.

Due to the form of the parameterizations, for the normal case Eq. (34) is reduced to an equation of the same type but with coefficients F_{1N}, F_{2N}, F_{3N} and F_{4N} which are different from F_1, F_2, F_3 and F_4. Furthermore, in the normal case, G_2, G_3, G_5, $\in$ and $\mathbf{v}^*$ are prescribed as observed normal values G_{2N}, G_{3N}, G_{5N}, $\in_N$ and $\mathbf{v}^*_{N_{ob}}$; and therefore, the model computes only the anomalies of these variables. For the normal and abnormal cases T'_m, T'_s, E_s, E_T, A_D and α are generated as full variables, except for T'_s in the oceans, where only the anomaly is computed, and where normal observed values are used for the normal case.

The boundary condition for (34) is $T_m' = T_{m_{ob}}' + (T_{m_B}' - T_{m_{NB}}')$ where $T_{m_{ob}}'$ is the normal observed temperature at the middle of the model's atmospheric layer; and T_{m_B}' and $T_{m_{NB}}'$ are, respectively, the abnormal and the normal solutions of (34) when the horizontal transport terms are neglected (i.e., $T_{m_B}' = F_4/F_3$ and $T_{m_{NB}}' = F_{4N}/F_{3N}$). Therefore, a variable boundary condition, which includes a computed anomaly, is used instead of a fixed one with zero anomaly.

To solve (34) we prescribe, besides the boundary conditions, the surface ocean and 700 mb temperatures in the previous interval (T_{sp}' and T_{mp}') and the initial surface albedo (α_p).

We start the computations in August. Both for the normal and the abnormal cases, we use as initial condition the observed July normal values of the surface ocean temperatures and the 700mb temperatures (T_{sp}' and T_{mp}'), and the surface albedo in August. For the ith month ($i > 1$) we use for T_{mp}' and α_p the 700mb temperature and the surface albedo computed in the i-1th month; and for T_{sp}' we use $(T_{sN_{ob}})_{i-1} + [(T_s)_{i-1} - (T_{sN})_{i-1}]$ where $(T_{sN_{ob}})_{i-1}$ is the normal observed surface ocean temperature in the i-1th month, and $(T_s)_{i-1}$ and $(T_{s_N})_{i-1}$ are the normal and abnormal ocean temperatures computed in the previous month, respectively.

The data, coefficients, region of integration and grid points used in the computations are described in previous papers (Adem 1964a,b; 1965b, 1970a,b). To obtain T_m', Eq. (34) is solved as a finite difference equation by the Liebmann relaxation method (Thompson, 1961). T_s' and the other variables are obtained by direct substitution of T_m' in the corresponding equations described above.

The computation of the feedback effect by atmospheric water vapor, explained in Section 6, would require an iterative procedure between the climate anomaly and the spectral increment; first the climate anomaly due to CO_2 doubling is computed without the water vapor feedback, which is used to compute the spectral increment; then a new anomaly is computed including this increment, and so on, until both the anomaly and the increment reach stable values. In order to abridge this iteration, we attempt to guess the final climate anomaly, and we test it for a consistent spectral increment; if not, we try another guess.

As we have seen, the climatic parameters needed to compute the atmospheric long wave spectrum, i.e. the absorptivities a_1, a_2, a_{12}, . . . a_{18} due to H_2O and CO_2, are T_a, P_a, β, $\in$ and H. In addition, only the atmospheric CO_2 content (U_B) is necessary to compute the spectrum. Using the normal present values of these 6 parameters (denoted with the subindex N) the basic spectrum is computed.

When a climatic change is externally forced, the absorptivities change due to the change in atmospheric H_2O content (U_A). Thus, the climate change is wholly characterized by the surface temperature anomaly (T_sDN), because the increments T_aDN, βDN and $\in DN$ are function only of T_sDN, when P_a and H remain fixed.

Our external forcing is the CO_2 doubling, i.e. $U_BDN = U_{B_N}$, or $U_B = 2U_{B_N}$, where variables with no subindexes mean abnormal values. In order to find the equilibrium anomaly T_sDN, we attempt a first guess $< T_sDN_{1g} >$, where $< >$ denotes the annual average over the total region of integration. We compute the corresponding values of $< T_aDN_{1g} >$, $< \beta DN_{1g} >$ and $< \in DN_{1g} >$, and introduce them in the formulas from Adem (1967), Smith (1969) and Ramanathan (1976), to compute the absorptivities a_i; this spectum is then used to compute T_sDN_1. If $< T_sDN_1 > \neq < T_sDN_{1g} >$, we try a new value $< T_sDN_{2g} >$ using a linear interpolation, and so on until $< T_sDN_i > = < T_sDN_{1g} >$.

8. RESULTS

The output of the model consists in a dozen of maps for each variable, for the months of the year. Here we show only the maps of the increase of surface temperature and precipitation due to a doubling of CO_2, for January, April, July and October, computed by means of the complete model including all feedbacks. These maps are presented in Figures 3A to 4D.

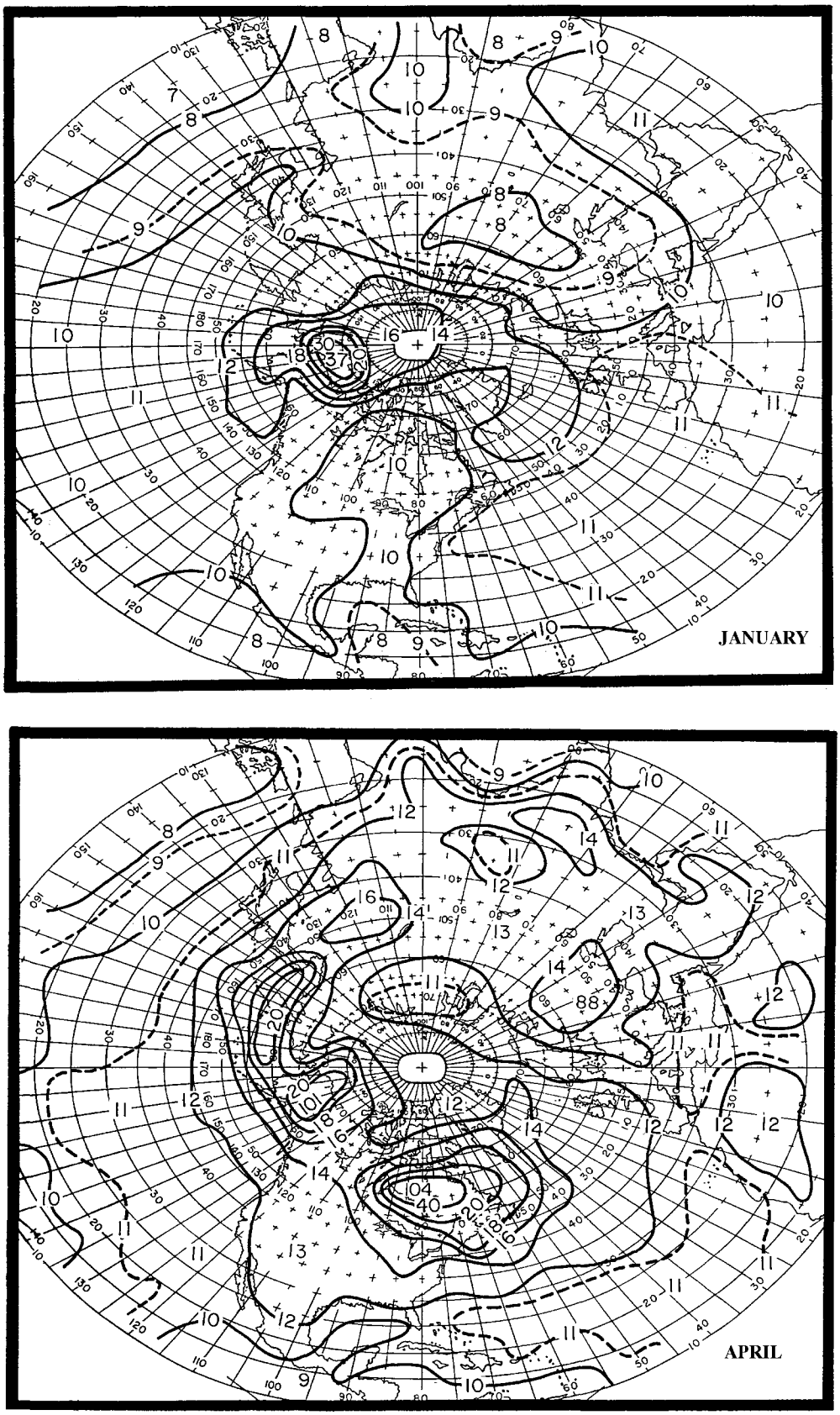

Fig. 3. Increase in the surface temperature for January (part A), April (B), July (C) and October (D), in tenths of ° C, due to a doubling of the atmospheric CO_2, computed with our model ATM1 (in which the water vapor acts in all the wave lengths of the atmospheric spectrum) for case 8 (with the three feedbacks included).

C

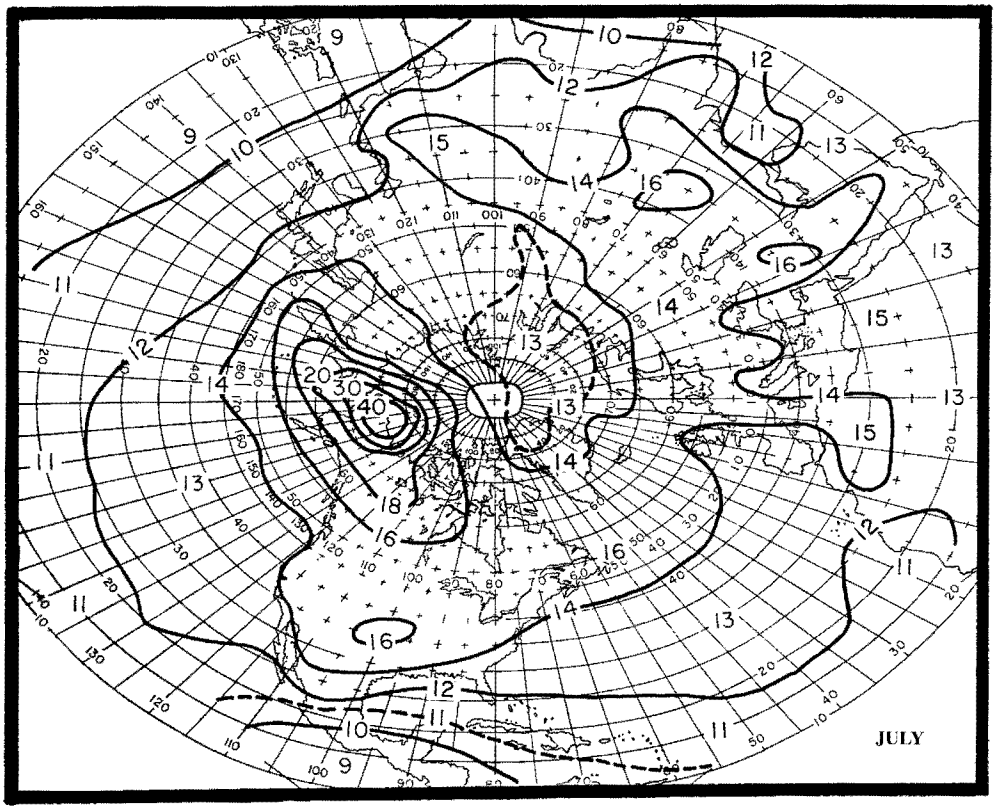

D

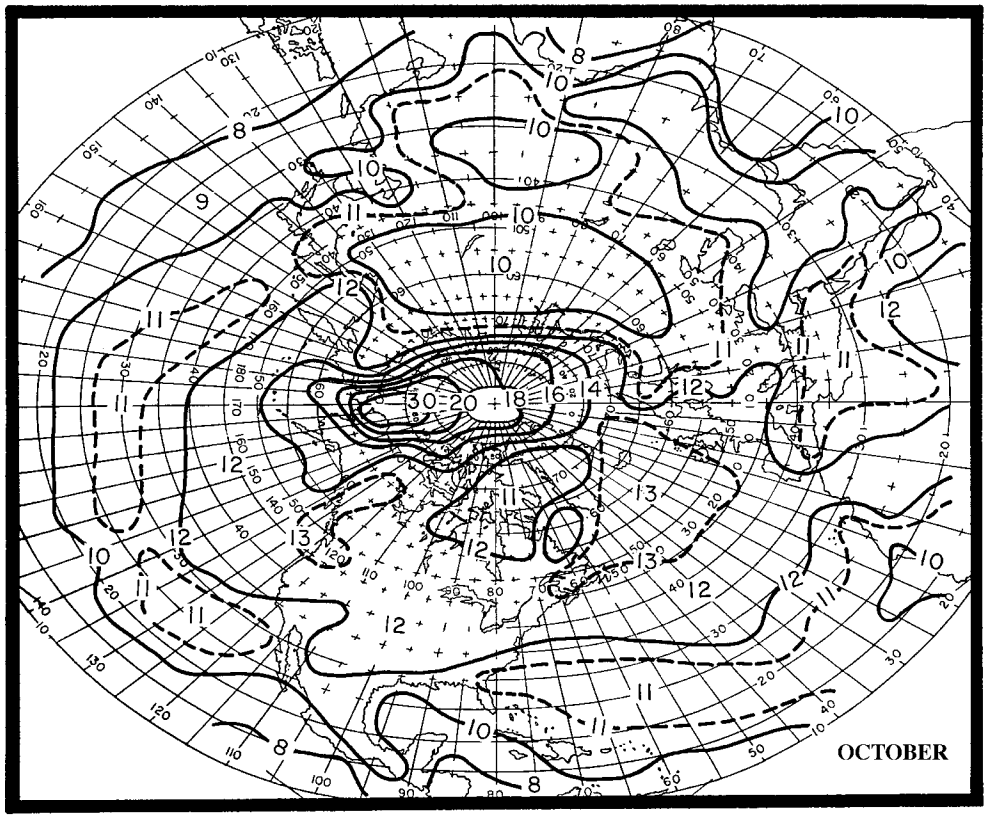

Fig. 3. (Cont.)

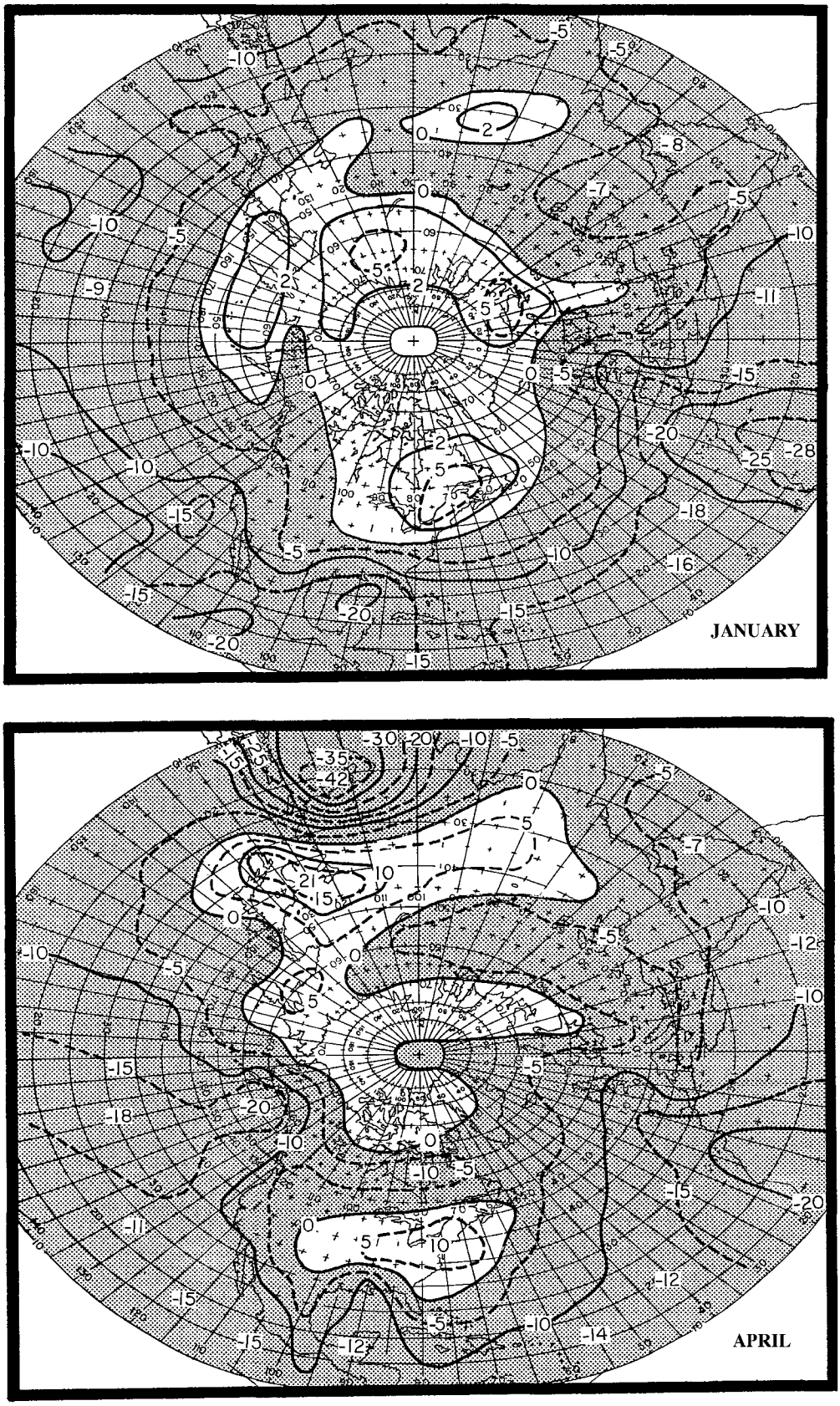

Fig. 4. Increase in the precipitation for January (part A), April (B), July (C) and October (D), in mm/month, due to a doubling of the atmospheric CO_2, computed with our model ATM1 (in which the water vapor acts in all the wave lengths of the atmospheric spectrum) for case 8 (with the three fedbacks included).

C

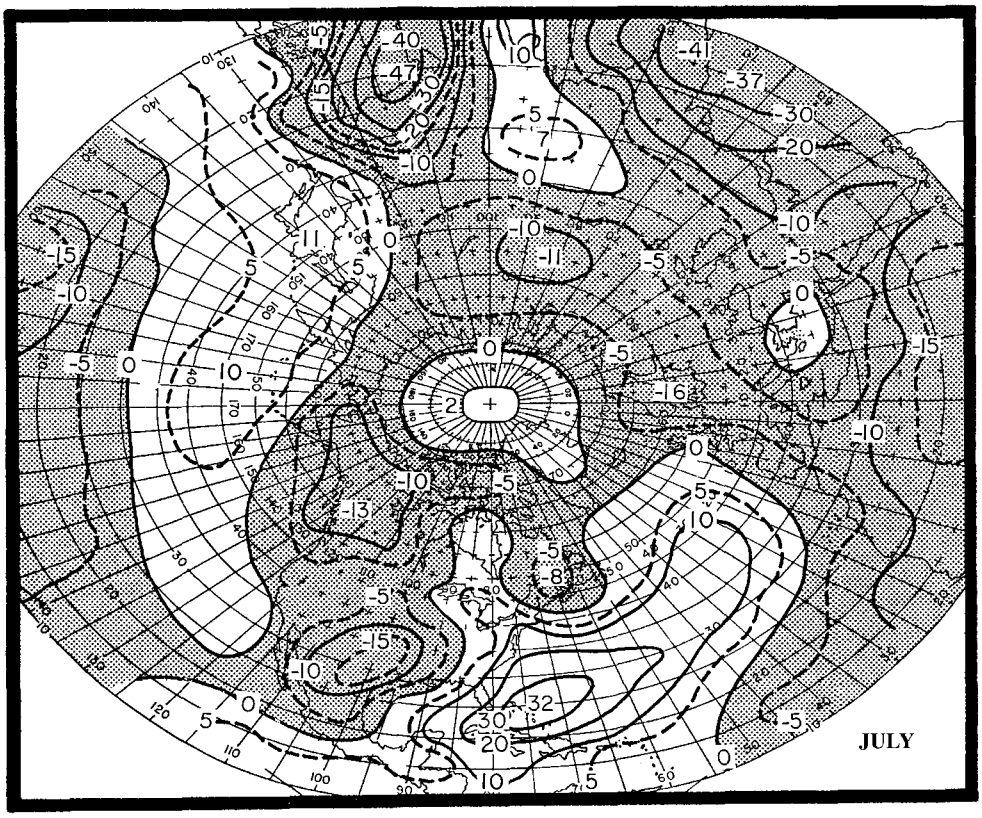

D

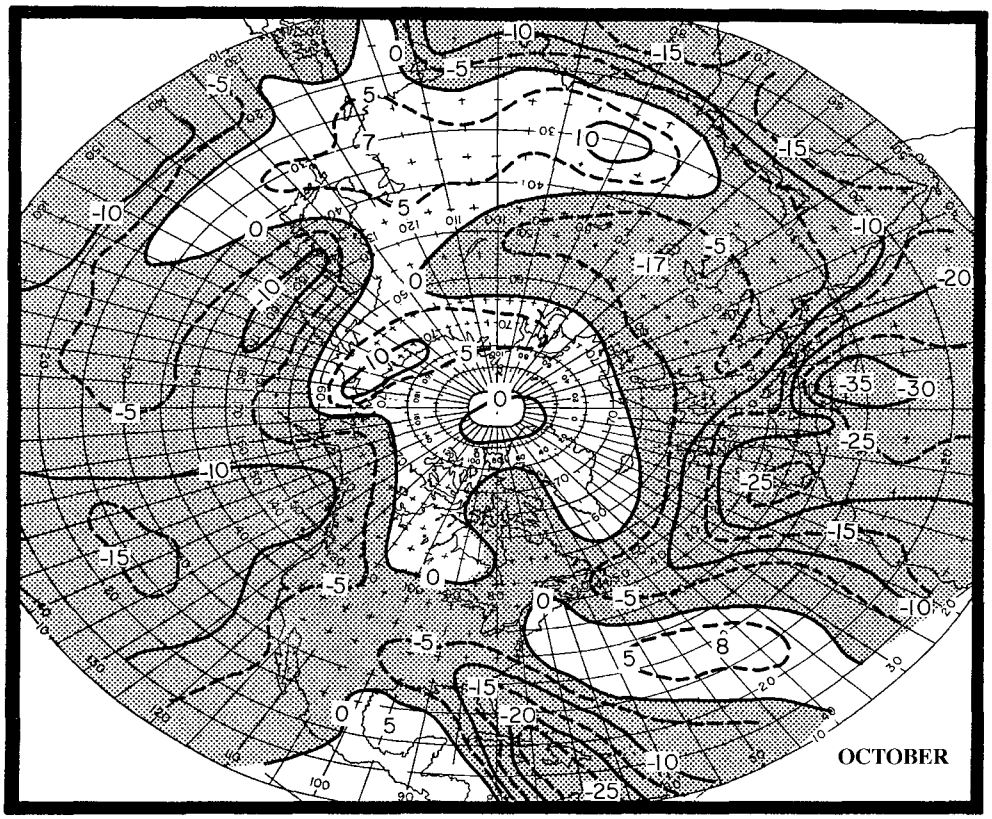

Fig. 4. (Cont.)

Table 1

Increase of surface temperature in °C and feedback factor due to doubling the atmospheric CO_2, resulting from our models (ATM1 and ATM2), and from the models of Hansen *et al*. (1984), and Schlesinger (1986), denoted HM and SM, respectively. Case 1 is without feedback mechanisms, case 8 includes the three (namely, the increases of water vapor, snow-ice and cloudiness), cases 2, 3 and 4 have one feedback and 5, 6 and 7 have two. ATM1 is our model with water vapor radiatively acting in all the wave lengths of the atmospheric spectrum, in ATM2 the water is absent from the band where the CO_2 acts (12-19μ). Feedback factor is defined as the ratio of the temperature increase in one case, divided by that of case 1. In the last column appears the ratio of temperature increase from one of our models by the other.

Case	Feedbacks included	Temperature increase (° C)				Feedback factor				
		ATM1	ATM2	HM	SM	ATM1	ATM2	HM	SM	ATM2/ ATM1
1	(ΔCO_2)	0.3	0.8	1.2	1.35	1	1	1	1	2.7
2	$+\Delta H_2O$	0.4	1.1	2.0	1.94	1.3	1.4	1.7	1.4	2.8
3	+Δcloud	0.4	1.3	1.6	1.38	1.3	1.6	1.3	1.0	3.3
4	+Δsnow/ice	0.4	1.2	1.3	1.56	1.3	1.5	1.1	1.2	3.0
5	$+\Delta H_2O$ + Δcloud	0.8	1.7	3.2	1.81	2.7	2.1	2.7	1.3	2.1
6	$+\Delta H_2O$ + Δsnow/ice	0.5	1.8		2.39	1.7	2.3		1.8	3.6
7	+Δcloud+Δsnow/ice	0.6	2.2			2.0	2.8			3.7
8	$+\Delta H_2O$+Δcloud+Δsnow/ice	1.2	3.5	4.2		4.0	4.4	3.5		2.9

In order to evaluate the feedback effects, we present a comparative study of the annual NH averages of the computed surface temperature increase (Table 1). The second column in the table specifies the feedback mechanisms, case 1 includes no feedback and case 8 includes all three feedbacks, namely increments of H_2O, snow-ice and clouds. The other cases include one or two feedback mechanisms.

The third column shows the temperature increase computed using the model with H_2O for all wavelengths of the emission spectrum, denoted by ATM1. When there is no feedback the increase of temperature is 0.3° C, and when the three mechanisms are included the increase is 1.2° C; for only one feedback the increase is 0.4° C in all three cases. When two feedbacks are included the increase is 0.8° C for the combination of H_2O plus clouds, 0.5° C for H_2O plus snow-ice, and 0.6° C for clouds plus snow-ice.

In the next column, called ATM2, we show the corresponding values for a model in which H_2O is absent in the CO_2 band. The increase is 0.8° C without any feedback and 3.5° C with all three mechanisms. When there is only one feedback the increase is 1.1, 1.3 and 1.2° C for H_2O (only in 0-12μ and 19μ–∞ bands), clouds, and snow-ice. When there are two feedbacks, the increase is 1.7, 1.8 and 2.2°C for the cases H_2O plus clouds, H_2O plus snow-ice and clouds plus snow-ice, respective.

In the fifth and sixth columns we find the corresponding values of surface air temperature increase as computed by Hansen *et al*. (1984), and by Schlesinger (1986). In the seventh, eighth, ninth and tenth columns we list the feedback factors defined as the quotient of the temperature increase in each case divided by that of case 1, for models ATM1, ATM2, HM and SM, respectively. A comparison of the four models shows that the factors are similar. Thus, the solutions are almost proportional to the temperature increases for case 1 (in which the feedback is excluded), namely, 0.3, 0.8, 1.2 and 1.35°C for ATM1, ATM2, HM and SM, respectively.

In cases 5, 6 and 7 when we have a combination of two feedbacks, inclusion of snow-ice (6 and 7) yields the largest factors for ATM2 and the smallest for ATM1, which suggests that the snow-ice effect depends non-linearly on the temperature change, since much larger feedback factors are obtained for larger increases of temperature.

The total feedback factor, which includes the three mechanisms and corresponds to case 8, is 4.0 and 4.4 for our

models ATM1 and ATM2, respectively, and 3.5 for HM.

The last column shows the ratio ATM2/ATMI. When H_2O is absent from the CO_2 band, the increase of temperature is about three times larger than when it is present. This strong difference is due to the radiative interaction of H_2O with CO_2, which reduces the net effect of doubling the CO_2. This reduction can be seen from the atmospheric emission spectra used in the model (Figure 2), where the shaded area is the energy emitted by the atmosphere for current CO_2 content, and the black area is the increase due to doubling the CO_2. Parts A and B are the emission spectra for CO_2 alone and for H_2O alone, respectively, and part C is the spectrum corresponding to the combined effect of both gases. The black area in the CO_2 band (12-19μ) is larger in the spectrum for CO_2 alone (part A) than for CO_2 and H_2O combined (part C), as the presence of H_2O in these interval reduces the effect of CO_2 doubling, because the spectrum of CO_2 plus H_2O gets closer to Planck's curve, and there is no room for larger increases in the spectrum. This saturation effect limits the temperature increase due to the increase of CO_2, as mentioned by other authors (Kiehl and Ramanathan, 1982; Ellsaesser, 1984, 1990; Lindzen, 1990).

Figure 1 presents the values obtained by several authors using different models. Hansen *et al*. (1984) value is number 35 and is one of the largest; our own earlier value (Adem and Garduño, 1984), is number 30, and our new one, falls in the same range, on the lower side of the solutions. Most values fall between the values obtained with our model, depending on whether the H_2O is present or absent in the CO_2 interval, i.e., 1.2° to 3.5° C. Considering that "the 12-18μ H_2O continuum absortion is neglected in most model studies" (Kiehl and Ramanathan, 1982), we conclude that the interaction of H_2O and CO_2 in this band could be a possible cause of the discrepancies in the values shown in this figure.

9. CONCLUSIONS

1. The feedback factors of the Adem Thermodynamic Model are similar to those of Hansen *et al*. (1984), and Schlesinger (1986), except for Schlesinger's cloudiness factor, which is very close to unity, and produces a relatively small effect. The feedback factor due to all three mechanisms (H_2O, snow-ice and clouds) is 4.0 and 4.4 for our model, and 3.5 for Hansen *et al*.

2. The presence of H_2O in the CO_2 band (12-19μ) prevents the increase of temperature due to the saturation of the band, because the combined effect of CO_2 and H_2O yields an absorptivity that approaches unity, as in the black body case.

3. While the feedback factors are similar, the increase of temperature due to a doubling of CO_2 is equal to 1.2° C when H_2O is present in the CO_2 band, and 3.5° C when there is no H_2O. The corresponding value of Hansen *et al*. is 4.2° C. The strong difference in these values appears to depend on the corresponding values (0.3, 0.8 and 1.2° C), obtained before the three feedbacks are applied, which depend crucially on the content of H_2O in the CO_2 band. In conclusion, one possible cause of the strong difference in the solutions obtained by different models could be the discrepancies in the amount and distribution of H_2O in the atmosphere, and specially in the treatment of the effect of H_2O in the CO_2 band from 12 to 19μ.

ACKNOWLEDGEMENTS

We are indebted to J. Zintzún, A. Aguilar, M. E. Grijalva, T. del Cid and R. Meza for their help in the preparation of this paper.

BIBLIOGRAPHY

ACKERMAN, T. P., 1979. On the effect of CO_2 on atmospheric heating rates. *Tellus, 31*, 115-123.

ADEM, J., 1962. On the theory of the general circulation of the atmosphere. *Tellus, 14*, 102-115.

ADEM, J., 1964a. On the normal thermal state of the troposphere-ocean-continent system in the Northern Hemisphere. *Geofís. Int., 4*, 3-32.

ADEM, J., 1964b. On the physical basis for the numerical prediction of monthly and seasonal temperatures in the troposphere-ocean-continent system. *Mon. Wea. Rev., 92*, 91-104.

ADEM, J., 1965a. Experiments aiming at monthly and seasonal numerical weather prediction. *Mon. Wea. Rev., 93*, 495-503.

ADEM, J., 1965b. Preliminary model for computing midtropospheric and surface temperatures from satellite data. *J. Geophys. Res., 70*, 376-386.

ADEM, J., 1967. Parameterization of atmospheric humidity using cloudiness and temperature. *Mon. Wea. Rev., 95*, 83-88.

ADEM, J., 1968. A parametric method for computing the mean water budget of the atmosphere. *Tellus, 20*, 621-632.

ADEM, J., 1070a. On the prediction of mean monthly ocean temperature. *Tellus, 22*, 410-430.

ADEM, J., 1970b. Incorporation of advection of heat by mean winds and by ocean currents in a thermodynamic model for long-range weather prediction. *Mon. Wea. Rev., 98*, 776-786.

ADEM, J., 1981. Numerical simulation of the annual cycle of climate during the ice ages. *J. Geophys. Res., 86*, 12015-12034.

ADEM, J., 1982. Simulation of the annual cycle of climate with a thermodynamic numerical model. *Geofís. Int., 21*, 229-243.

ADEM, J. and R. GARDUÑO, 1982. Preliminary experiments on the climatic effect of an increase of the atmospheric CO_2 using a thermodynamic model. *Geofís. Int., 21*, 309-324.

ADEM, J. and R. GARDUÑO, 1984. Sensitivity studies on the climatic effect of an increase of atmospheric CO_2. *Geofís. Int., 23*, 17-35.

AUGUSTSSON, T. and V. RAMANATHAN, 1977. A radiative convective model study of the CO_2 climate problem. *J. Atmos. Sci., 24*, 448-451.

CHARLOCK, T. P., 1981. Cloud optics as a possible stabilizing factor in climate change. *J. Atmos. Sci., 38*, 661-663.

CHOU, M. D., L. PENG and A. ARKING, 1982. Climate studies with a multilayer energy balance model, Part II: the role of feedback mechanisms in the CO_2 problem. *J. Atmos. Sci., 39*, 2657-2666.

CLAPP, P. F., S. H. SCOLNIK, R. E. TAUBENSEE , and F. J. WINNINHOFF, 1965. Parameterization of certain atmospheric heat sources and sinks for use in a numerical model for monthly and seasonal forecasting. Unpublished study of Extended Forecast Division, U. S. Weather Bureau, Washington, D. C. (copies available for interested persons).

CLAPP, P. F., 1970. Parameterization of macroscale transient heat transport for use in a mean-motion model of the general circulation. *J. Appl. Meteorol., 9*, 554-563.

DEFANT, A., 1921. Die Zirkulation der Atmosphäre in den gemässigten Breiten der Erde. *Geog. Ann., 3*, 209-266.

ELLSAESSER, H. W., 1984. The climatic effect of CO_2: A different view. *Atmos. Environ., 18*, 431-434.

ELLSAESER, H. W., 1990. A different view of the climatic effect of CO_2 - Updated. *Atmósfera, 3*, 3-29.

GARDUÑO, R. and J. ADEM, 1988. Interactive long wave spectrum for the thermodynamic model. *Atmósfera, 1*, 157-172.

GARDUÑO, R. and J. ADEM, 1993. Parameterization of cloudiness as a function of temperature for use in a thermodynamic model. *World Resource Review, 5*, 246-253.

GUTOWSKI, W. J., W. C. WANG and P. H. STONE, 1985. Effects of dynamic heat fluxes on model climate sensitivity: meridional sensible and latent heat fluxes. *J. Geophys. Res., 90(D7)*, 13081-13086.

HANSEN, J., D. JOHNSON, A. LACIS, S. LEBEDEFF, P. LEE, D. RIND and G. RUSSELL, 1981. Climate impact of increasing atmospheric carbon dioxide. *Science, 213*, 957-966.

HANSEN, J., A. LACIS, D. RIND, G. RUSSELL, P. STONE, I. FUNG, R. RUEDY and J. LERNER, 1984. Climate sensitivity: analysis of feedback mechanisms. *In:* Climate processes and climate sensitivity. Eds.: J. E. Hansen and T. Takahashi, Maurice Ewing series 5. American Geophysical Union, Washington, D. C. 130-163.

HUMMEL, J. R., 1982a. Surface temperature sensitivities in a multiple cloud radiative-convective model with a constant and pressure dependent lapse rate. *Tellus, 34*, 203-208.

HUMMEL, J. R., 1982b. Anomalous water-vapor absorption: implications for radiative-convective models. *J. Atmos. Sci., 39*, 879-885.

HUMMEL, J. R. and W. R. KUHN, 1981a. Comparison of radiative-convective models with constant and pressure dependent lapse rates. *Tellus, 33*, 254-261.

HUMMEL, J. R. and W. R. KUHN, 1981b. An atmospheric radiative-convective model with interactive water vapor transport and cloud development. *Tellus, 33*, 372-381.

HUMMEL, J. R. and R. A. RECK, 1981. Carbon dioxide and climate: the effects of water transport in radiative-convective models. *J. Geophys. Res., 86* (C12), 12035-12038.

HUNT, B. G., 1981. An examination of some feedback mechanisms in the carbon dioxide climate problem. *Tellus, 33*, 78-88.

HUNT, B. G. and N. C. WELLS, 1979. An assessment of the possible future climate impact of carbon dioxide increases based on a coupled one-dimensional atmospheric-oceanic model. *J. Geophys. Res, 84*, 787-791.

KIEHL, J. T. and V. RAMANATHAN, 1982. Radiative heating due to increased CO_2: the role of H_2O continuum absorption in the 12-18 μm region. *J. Atmos. Sci., 39*, 2923-2926.

LAL, M. and V. RAMANATHAN, 1984. The effects of moist convection of water vapor radiative processes on climate sensitivity. *J. Atmos. Sci., 41*, 2238-2249.

LINDZEN, R. S., 1990. Some coolness concerning global warming. *Bull. Am. Meteor. Soc., 71*, 288-299.

LINDZEN, R. S., A. Y. HOU and B. F. FARRELL, 1982. The role of convective model choice in calculating the climate impact of doubling CO_2. *J. Atmos. Sci., 39*, 1189-1205.

MANABE, S., 1971. Estimate of future changes in climate due to increase of carbon dioxide concentration in the air. *In:* Man's impact on the climate, Eds. W. H. Mathews, W. W. Kellogg and G. D. Robinson, MIT Press, Cambridge, Massachusetts. 249-264.

MANABE, S. and R. T. WETHERALD, 1967. Thermal equilibrium of the atmosphere with a given distribution of relative humidity. *J. Atmos. Sci., 24*, 241-159.

MANABE, S. and R. T. WETHERALD, 1975. The effect of doubling the CO_2 concentration on the climate of a general circulation model. *J. Atmos. Sci., 32*, 3-15.

MANABE, S. and R. T. WETHERALD, 1980. On the distribution of climate change resulting from an increase in CO_2-content of the atmosphere. *J. Atmos. Sci., 37*, 99-118.

OHRING, G. and S. ADLER, 1978. Some experiments with a zonally averaged climate model. *J. Atmos. Sci., 35*, 186-205.

OU, S. C. S. and K. N. LIOU, 1985. Cumulus convection and climatic temperature perturbation. *J. Geophys. Res., 90 (D1)*, 2223-2232.

POTTER, G. L., 1980. Zonal model calculation of the climatic effect of increased CO_2. *In:* Environmental and climatic impact of coal utilization, Eds. J. J. Singh and A. Deepak, Academic Press, New York, 433-454.

RAMANATHAN, V., 1976. A radiative transfer within the Earth's troposphere and stratosphere: a simplified radiative-convective model. *J. Atmos. Sci., 33*, 1330-1346.

RAMANATHAN, V., 1981. The role of ocean-atmosphere interactions in the CO_2 climate problem. *J. Atmos. Sci., 38*, 918-930.

RAMANATHAN, V., M. S. LIAN and R. D. CESS, 1979. Increased atmospheric CO_2: zonal and seasonal estimates of the effect on the radiation energy balance and surface temperature. *J. Geophys. Res., 84*, 4949-4958.

RASOOL, S. I. and S. H. SCHNEIDER, 1971. Atmospheric carbon dioxide and aerosols: effects of large increases on global climate. *Science, 173*, 138-141.

ROWNTREE, P. R. and J. WALKER, 1978. The effects of doubling the CO_2 concentration on radiative-convective equilibrium. *In:* Carbon dioxide, climate and society, Ed. J. Williams, Pergamon, Oxford, 181-191.

SCHLESINGER, M. E., 1983. A review of climate model simulations of CO_2-induced climatic change, Rep. 41, Climatic Research Institute, Oregon State University, Corvallis.

SCHLESINGER, M. E., 1984. Climate model simulation of CO_2-induced climatic change. *Adv. Geophys., 26*, 141-235.

SCHLESINGER, M. E., 1986. Equilibrium and transient climatic warming induced by increased atmospheric CO_2. *Clim. Dyn., 1*, 35-51.

SMITH, W. L., 1969. A polynomial representation of carbon dioxide and water vapor transmission. ESSA Tech. Rep. NESC 47.

SOMERVILLE, R. C. J. and L. A. REMER, 1984. Cloud optical thickness feedbacks in the CO_2 climate problem. *J. Geophys. Res., 89 (D6)*, 9668-9672.

TEMKIN, R. L. and F. M. SNELL, 1976. An annual zonally-averaged hemispherical climate model with diffuse cloudiness feedback. *J. Atmos. Sci., 33*, 1671-1685.

THOMPSON, P. D., 1961. Numerical weather analysis and prediction, Macmillan, New York.

TRICOT, Ch. and A. BERGER, 1987. Modelling the equilibrium and transient responses of global temperature to past and future trace gas concentrations. *Clim. Dyn., 2*, 39-61.

WANG, W. C. and P. H. STONE, 1980. Effect of ice-albedo feedback on global sensitivity in a one-dimensional ra-

diative-convective climate model. *J. Atmos. Sci., 37*, 545-552.

WANG, W. C, W. B. ROSSOW, N. S. YAO and M. WOLFSON, 1981. Climate sensitivity of a one-dimensional radiative-convective model with cloud feedback. *J. Atmos. Sci., 38*, 1167-1178.

WANG, W. C., G. MOLNAR, T. D. MITCHELL and P. H. STONE, 1984. Effects of dynamical heat fluxes on model climate sensitivity. *J. Geophys. Res., 89*, (D3), 4699-4711.

WASHINGTON, W. M. and G. A. MEEHL, 1983. General circulation model experiment on the climatic effects due to a doubling and quadrupling of carbon dioxide concentration. *J. Geophys. Res., 88*, 6600-6610.

WASHINGTON, W. M. and G. A. MEEHL, 1984. Seasonal cycle experiment on the climate sensitivity due to a doubling of CO_2 with an atmospheric general circulation model coupled to a simple mixed-layer ocean model. *J. Geophys. Res., 89*, (D6), 9475-9503.

WEARE, B. C. and F. M. SNELL, 1974. A diffuse thin cloud structure as a feedback mechanism in global climatic modeling. *J. Atmos. Sci., 31*, 1725-1734.

WETHERALD, R. T. and S. MANABE, 1986. An investigation of cloud cover change in response to thermal forcing. *Clim. Change, 8*, 5-23.

YAMAMOTO, G. and T. SASAMORI, 1958. Calculation of the absorption of the 15μ carbon dioxide band. Sci. Rep. Tohoku Univ., Fifth Ser. 10, No. 2.

YAMAMOTO, G. and T. SASAMORI, 1961. Further studies on the absorption of the 15μ carbon dioxide band. Sci. Rep. Tohoku Univ., Fifth Ser. 12, No. 1.

Julián Adem[1,2] and René Garduño[2]

[1] *Member of El Colegio Nacional, México.*

[2] *Centro de Ciencias de la Atmósfera, UNAM, CU, 04510 México, DF, México.*